

## STRUCTURAL ANALYSIS OF PLATE-SHAPED PRECIPITATES IN NEUTRON IRRADIATED V-4Cr-4Ti - D.T. Hoelzer and S.J Zinkle (Oak Ridge National Laboratory)

### OBJECTIVE

To investigate the mechanisms of migration, segregation, and precipitation of the interstitial elements (C, O, N) in vanadium alloys during thermomechanical treatments, welding, neutron irradiation, and exposure to oxidizing environments.

### SUMMARY

Neutron irradiation of V-4Cr-4Ti at  $\sim 510^\circ\text{C}$  and dose of  $\sim 4$  dpa resulted in the formation of a relatively high number density of plate shaped precipitates on  $\{100\}_{\text{bcc}}$  habit planes. The TEM analysis showed that their average size was  $\sim 24$  nm ( $\pm 12$  nm) in diameter and  $\sim 1$ -3 nm in thickness. Diffuse streaking from the precipitates was observed to lie parallel to  $\langle 100 \rangle_{\text{bcc}}$  directions and centered at  $3/4\langle 200 \rangle$  positions in electron diffraction patterns. Based on an orientation relationship observed between the precipitates and bcc matrix and a tilting experiment on one plate variant, the structural analysis indicated that the crystal structure of the plates was consistent with the fcc structure, which is the same for the globular-shaped Ti-(OCN) phase. The analysis also showed that diffuse scattering observed at  $2/3\langle 222 \rangle$  positions in electron diffraction patterns is not caused by the plate shaped phase.

### PROGRESS AND STATUS

#### Introduction

The results obtained in this study were from a V-4Cr-4Ti alloy that was incorporated in the varying temperature irradiation experiment (HFIR 13J) performed under the framework of the Japan-USA Program of Irradiation Tests for Fusion Research (JUPITER) [1-3]. This experiment was designed to study the effects of temperature variation on the microstructure and mechanical properties of candidate fusion reactor structural materials.

Several recent studies have shown that Ti-rich precipitates form with a plate shaped morphology in vanadium alloys containing Ti. This result has been observed for a variety of experimental conditions that include, (1) annealing at  $500^\circ\text{C}$  in a low oxygen pressure environment followed by annealing at  $950^\circ\text{C}$  [4], (5) post gas tungsten arc weld heat treatment at  $950^\circ\text{C}$  [5], and (6) neutron irradiation at low doses and temperatures  $>315^\circ\text{C}$  (HFBR) [6], 18 dpa and  $600^\circ\text{C}$  (DHCE) [7], 4dpa and  $\sim 390^\circ$  (EBR-II X530) [8], 13-27dpa and  $430$ - $600^\circ\text{C}$  (FFTF-DHCE) [8], and 14-40dpa and  $\sim 400$ - $600^\circ\text{C}$  (FFTF/MOTA) [9,10]. It is reasonable to assert based on these studies that the precipitates form on  $\{100\}$  planes in the bcc matrix [6], are associated with diffuse streaks in electron diffraction patterns such as a radial streak in the  $\langle 100 \rangle_{\text{bcc}}$  direction at  $\sim 3/4\langle 200 \rangle$  position and possibly a tangential streak at  $\sim 2/3\langle 222 \rangle$  position [7], and are Ti-rich containing interstitial solute atoms [4-6]. However, there still exists considerable uncertainty about the crystal structure, composition, and morphology of these precipitates, especially at particle sizes in the nanometer range. For example, nano-size precipitates were observed in neutron irradiated V-(4-5)Cr-(4-5)Ti at  $400^\circ\text{C}$  that were determined by PEELS to be Ti-rich, but the structure could not be unambiguously identified nor could the diffuse streaks observed at  $3/4\langle 200 \rangle$  and  $2/3\langle 222 \rangle$  be assigned to one or two types of precipitates [11]. Therefore, the purpose of this study is to develop a better understanding of the structure and crystallography of the plate shaped precipitates that form in vanadium alloys containing Ti, such as V-4Cr-4Ti.

## Experimental Procedure

Details of the JUPITER HFIR 13J variable temperature experiment have been published [1-3]. The TEM results of this study were from the V-4Cr-4Ti (Wah Chang heat #832665) that was neutron irradiated at an average temperature of 510°C (+/- 10°C) and dose of ~4 dpa.

## Results

The microstructure of the neutron irradiated V-4Cr-4Ti alloy consisted of the bcc V-rich matrix phase, an inhomogeneous distribution of prior globular-shaped Ti-OCN particles, and a homogeneous distribution of small plate-shaped precipitates with a relatively high number density of  $\sim 4.2 \times 10^{21}/\text{m}^3$ . The plate-shaped precipitates were associated with diffuse electron scattering that was observed as streaks lying parallel to  $\langle 100 \rangle_{\text{bcc}}$  in selected area electron diffraction (SAED) patterns. Figure 1 shows the bright field (BF) and dark field (DF) micrographs of the precipitates. The inset in Figure 1b shows the diffuse streak (marked by the arrow head) that was used to form the DF image. For these micrographs, the sample was oriented between the  $[001]_{\text{bcc}}$  and  $[011]_{\text{bcc}}$  zone axes and the diffuse streak associated with the plates was observed near  $3/4\langle 200 \rangle$  position. The analysis of the plates showed them to have an average diameter of 24 nm (+/- 12 nm) and a thickness typically less than 2-3 nm.

Figure 2 shows the plate-shaped precipitates with the thin foil specimen oriented along the  $[001]_{\text{bcc}}$  zone axis. At this orientation, two rotational variants of the plates are observed edge on and appear as rods in the projected image of Figure 2a. Both plate variants contain an  $\{001\}_{\text{bcc}}$  habit plane. The SAED pattern shown in Figure 2b was obtained by tilting slightly off the precise  $[001]_{\text{bcc}}$  zone axis in order to emphasize the diffuse streaking pattern from a single plate variant, i.e. the plate lying parallel to  $(100)_{\text{bcc}}$  in Figure 2a. This slight tilting resulted in a symmetrical pattern of diffuse streaks with each lying parallel to the  $\langle 100 \rangle$  directions. Along with the streak marked  $3/4\langle 200 \rangle$ , a similar streak exists closer to the 110 reflection and another one is superimposed on the 020 reflection.

Focusing on the  $(100)_{\text{bcc}}$  plate variant, SAED patterns were then obtained at the  $[011]$  and  $[111]$  zone axes and are shown in Figure 3. This was accomplished by tilting the thin foil specimen normal to the  $\langle 100 \rangle_{\text{bcc}}$  diffuse streaks, i.e. using  $g=200_{\text{bcc}}$ , from  $B=[001]$  to  $B=[011]$  ( $45^\circ$  tilt) and then from  $B=[011]$  to  $B=[111]$  ( $\sim 35^\circ$  tilt). A systematic row of diffuse streaks associated with the

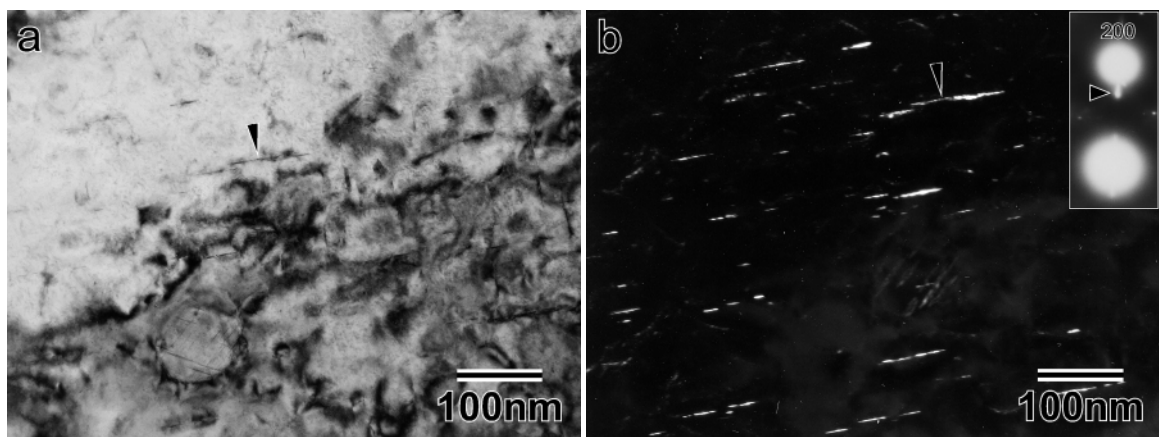


Figure 1. TEM micrographs showing the plate shaped precipitates that formed in the neutron irradiated V-4Cr-4Ti. (a) bright field and (b) dark field using diffuse streak at  $g = 3/4\langle 200 \rangle$ .

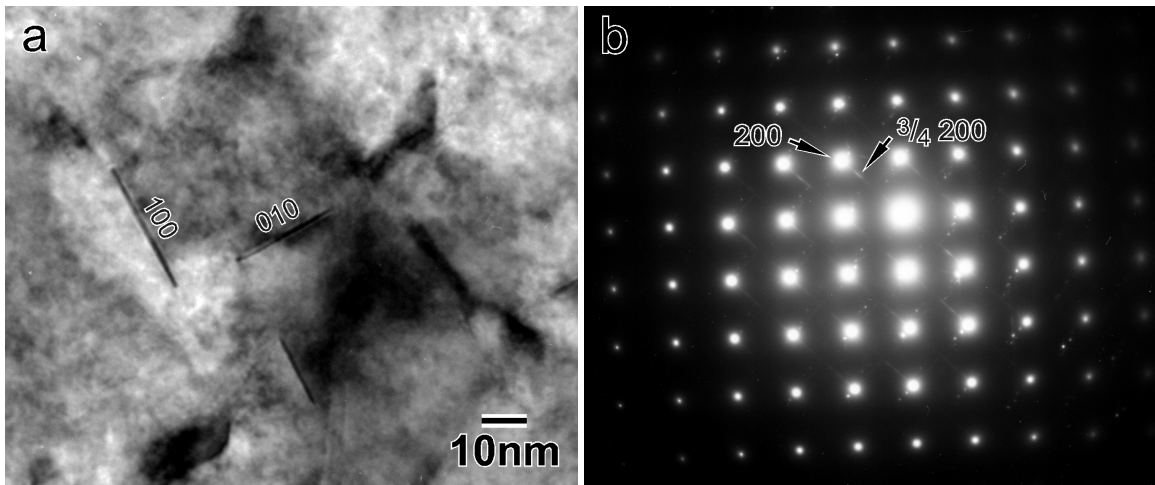


Figure 2. (a) TEM bright field micrograph showing two plate variants with (100) and (010) habit planes and (b) SAED pattern showing the diffuse streaking pattern for the (100) plate variant at the slightly tilted off axis  $[001]_{\text{bcc}}$  zone axis.

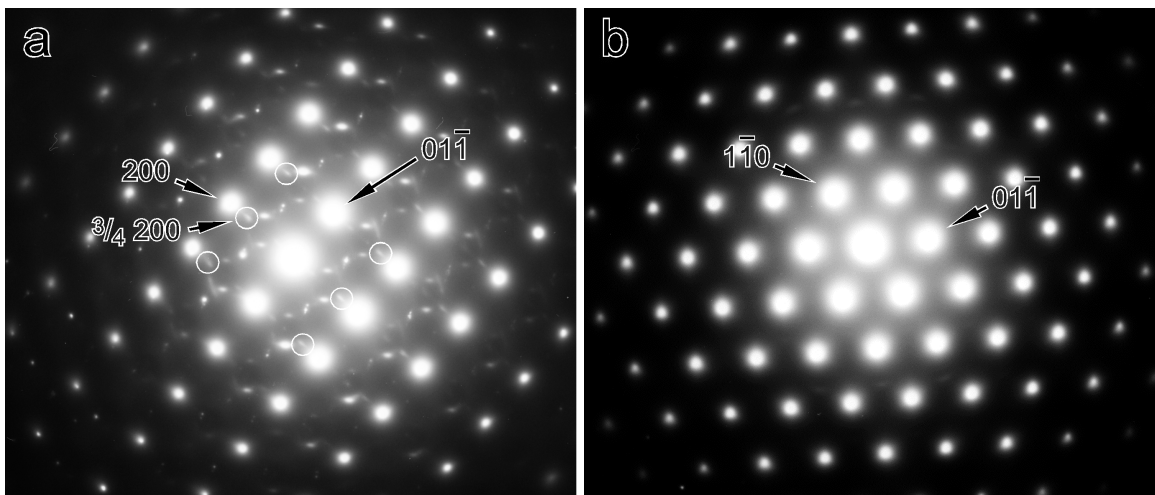


Figure 3. SAED patterns showing the diffuse streaking pattern for the (100) plate variant that was observed at (a) the  $[011]_{\text{bcc}}$  zone axis and (b) the  $[111]_{\text{bcc}}$  zone axis.

(100) plate variant are observed at the  $[011]_{\text{bcc}}$  zone axis as shown in Figure 3a. These streaks are enclosed in circles. Additional diffuse scattering signals are also observed at the  $[011]_{\text{bcc}}$  zone axis including the diffuse arcs at  $\sim 2/3 \langle 222 \rangle$ . However, tilting to the  $[111]_{\text{bcc}}$  zone axis along  $g=01\bar{1}$  resulted in no apparent visible diffuse streaks as shown in Figure 3b.

### Discussion

The results showed that neutron irradiation at  $\sim 510^\circ\text{C}$  and dose of  $\sim 4$  dpa resulted in the formation of a relatively high number density of plate shaped precipitates. Although no compositional data was obtained at the time of this report, the observation of diffuse streaks in

electron diffraction patterns and the  $\{100\}_{\text{bcc}}$  habit plane indicate that these precipitates are consistent with Ti-rich plates reported from previous studies [5,6]. In a recent study [12], a similar morphology and crystallography was observed for plates that formed in oxygen doped V-4Cr-4Ti annealed at 950°C [4] and analysis by EELS and EDS showed them to be Ti-rich containing varying levels of C, O and N. The same type of compositional analysis will be performed on the plates observed in the neutron irradiated specimen.

The crystal structure of the plate shaped phase was investigated by analyzing electron diffraction patterns recorded in the tilting experiment on one plate variant and comparing them with simulated diffraction patterns. The SAED pattern shown in Figure 1b indicates that an orientation relationship (OR) exists between the plate shaped phase and the bcc matrix. Since the intensity profile causing the diffuse streak is due to the phase shape factor, a maximum occurs near the center of the streak. The location of the intensity maximum was used for calculating the d-spacings, which are listed in Table 1 for several  $\langle 100 \rangle$  streaks at the  $[001]_{\text{bcc}}$  zone axis. The streak that lies normal to  $g=020_{\text{bcc}}$  is superimposed on the  $020_{\text{bcc}}$  reflection and can be confirmed by constructing a line that connects the center of streaks located near  $200_{\text{bcc}}$  and  $1\bar{1}1_{\text{bcc}}$ , which intersects the  $020_{\text{bcc}}$ . A reasonable correlation with the fcc crystal structure was then made based on self-consistencies in the measured d-spacings, interplanar angles, and structure factor considerations, i.e. using the (hkl) ratio method. Thus, the OR shown in Figure 1b was indexed as the  $[011]_{\text{fcc}}$  zone axis for the precipitates. From this result, the OR was consistent with  $[001]_{\text{m}} // [011]_{\text{p}}$  and  $(200)_{\text{m}} // (200)_{\text{p}}$ , where the subscript m is for matrix and p is for precipitate. This OR is the same as the Baker-Nutting OR [13] and has been observed for TiO precipitates in V-Ti alloys [14]. Finally, the lattice parameter of the fcc structure was calculated from the (hkl) assignments of the measured d-spacings and was found to be  $a=0.419$  (+/- 0.010 nm).

Simulated electron diffraction patterns were generated using DiffractII v1.2a (1990) in order to understand the diffuse streaking patterns recorded at  $[001]_{\text{bcc}}$  and  $[011]_{\text{bcc}}$  zone axes for the single plate variant used in the tilting experiment. Input crystallographic parameters were based on the lattice parameter calculated for the bcc matrix and fcc precipitate phase and the OR observed at the  $[001]_{\text{bcc}}$  zone axis. Figure 4 shows the results of the simulation taking into account two rotational plate variants, i.e. the plates observed on (100) and (010) habits in Figure 2a, and the plate shape factor. Figure 4a shows that the simulation accurately predicts the location of the intensity maxima, assuming a spherical shape, and also the direction of the intensity profile, or streak, when the plate shape factor is applied to the two plate variants at the  $[001]$  zone axis. At the  $[011]_{\text{bcc}}$  zone axis shown in Figure 4b, a systematic row of streaks appear in the  $\langle 100 \rangle$  direction at  $\sim 3/4 \langle 2xx \rangle$ , where  $x=0,1,2,..n$ , and another row of streaks intersect the matrix reflections at  $x00$ , where  $x=0,2,4,..even$ . Indexing these streaks is consistent with the  $[010]_{\text{fcc}}$  zone axis for the (100) plate variant used in the tilting experiment. The (010) plate variant lies 45° to the  $[011]_{\text{bcc}}$  zone axis and does not contribute to diffuse streak patterns in the SAED pattern (Figure 3a). However, it is possible that rel-rods caused by the plate shape factor may extend from higher order Laue zones and intersect the Ewald sphere. This possibility as well as double diffraction effects may account for the extra diffuse scattering phenomena that was observed at the  $[011]_{\text{bcc}}$  zone axis. Finally, the simulated pattern observed in Figure 4c indicates that the

Table 1. Structural analysis of the plate shaped precipitates.

Number	$\langle 100 \rangle$ Streak	d-spacing (+/- 0.002 nm)	(hkl) (fcc basis)	Ratio (Number reference)	
1	near 111	0.242	111	1.180 (1/2)	1.592 (1/3)
2	near 200	0.205	200	1.349 (2/3)	---
3	superimposed on 020	0.152	220	---	---

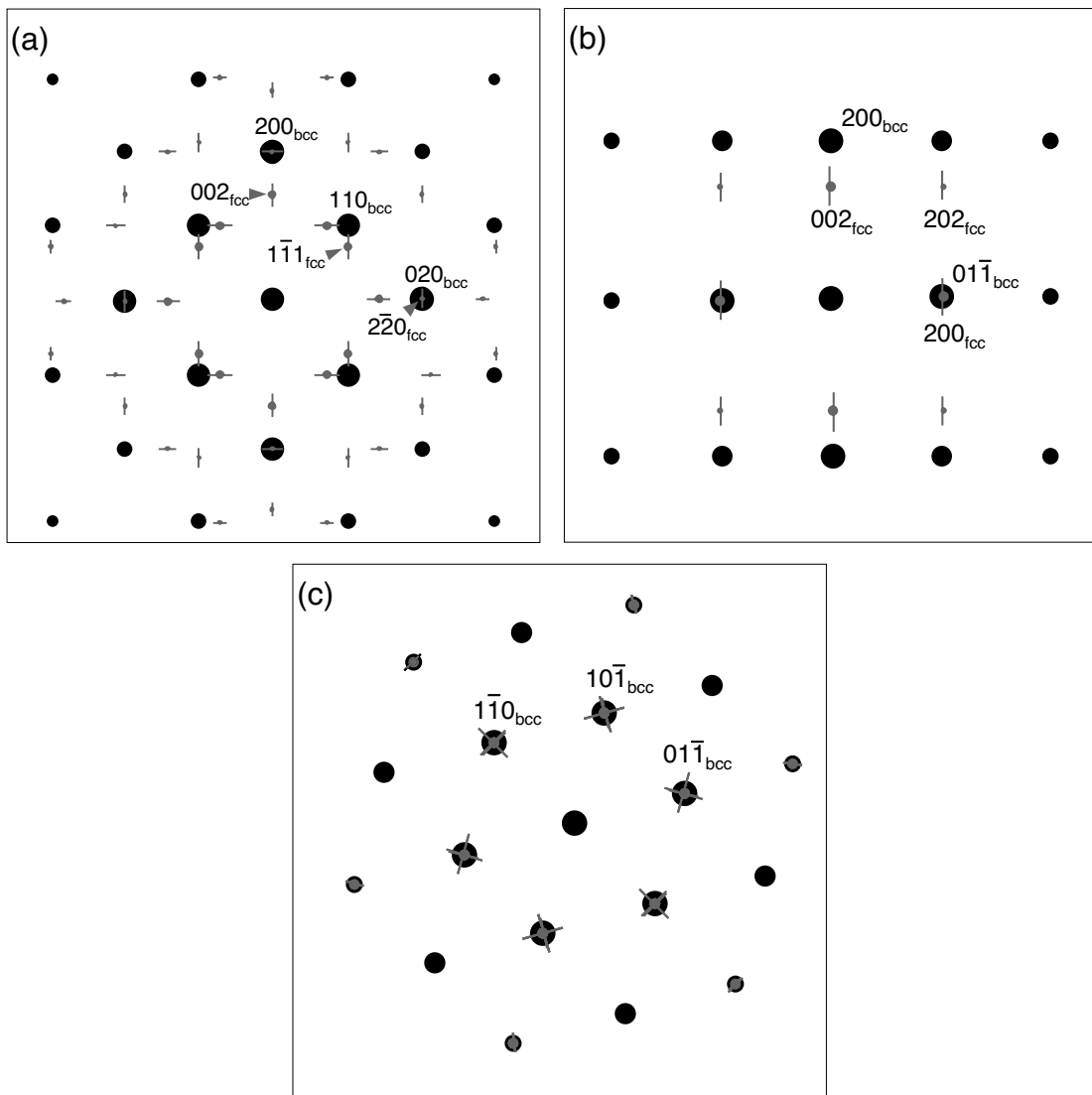


Figure 4. Simulated electron diffraction patterns showing the diffuse scattering patterns of the (100) and (010) plate variants at: (a)  $B=[001]_{\text{bcc}}$ , (b)  $B=[011]_{\text{bcc}}$ , and (c)  $B=[111]_{\text{bcc}}$  zone axes.

streaks from both plate variants are superimposed on matrix reflections and that this explains why no diffuse scattering was observed at the  $[111]_{\text{bcc}}$  zone axis in Figure 3c. From the OR, there are no low indice zone axes of the fcc phase for any rotational plate variant that coincide with the  $[111]_{\text{bcc}}$  zone axis. Thus, the agreement between SAED and simulated patterns is consistent with the fcc structure for the plate shaped precipitates, which is the same structure as the Ti-rich (OCN) phase [15].

The simulated electron patterns showed that there was no relationship between the Ti-rich plate shaped phase and the diffuse streaks, or arcs, that occur at the  $\sim 2/3\langle 222 \rangle$  position. These diffuse arcs have typically been observed at the  $\langle 011 \rangle_{\text{bcc}}$  zone axis [6,7] and are observed in the  $[011]_{\text{bcc}}$  zone axis of the SAED pattern shown in Figure 3a. This conclusion was based on

investigating the diffuse scattering behavior from all three rotational  $\{100\}$  plate variants at the  $[011]_{\text{bcc}}$  zone axis and changing the foil thickness as well as plate thickness in order to account for the diffuse arcs. No combination of parameters or variants could simulate the  $2/3\langle 222 \rangle$  diffuse arcs. Thus, it is concluded based on these results that the diffuse scattering at  $2/3\langle 222 \rangle$  is due to a different phase than the Ti-rich plate shaped phase. A similar conclusion was also obtained from the TEM analysis of the defect structures in neutron irradiated V-4Cr-4Ti at a dose of 19dpa and  $\sim 323^\circ\text{C}$  (BOR-60 FUSION experiment); diffuse arcs at  $2/3\langle 222 \rangle$  positions were observed but diffuse streaks at  $3/4\langle 200 \rangle$  positions were not observed in SAED patterns [16]. Preliminary results indicate that the diffuse arcs at  $2/3\langle 222 \rangle$  positions are due to surface contamination that occurs during thin foil preparation.

The results of this and other previous studies indicate that Ti-rich plates form in V-based alloys containing Ti in both neutron irradiated and unirradiated thermally aged conditions with no significant differences in structure and crystallography. However, differences in the experimental conditions could affect the formation temperature of the Ti-rich plates. The rate limiting parameter for precipitation under normal unirradiated conditions is the diffusion of solute Ti atoms. Since long-range diffusion of solute Ti atoms does not occur below  $500^\circ\text{C}$  in unirradiated V-alloys [17], this result implies that the Ti-rich plates will form only at temperatures higher than  $500^\circ\text{C}$  or after very long time at temperatures slightly above  $500^\circ\text{C}$  in the unirradiated condition. Alternatively, solute Ti atoms could interact with point defects generated during neutron irradiation, enhancing their diffusion rate and subsequently the precipitation of plates at temperatures below  $500^\circ\text{C}$  or above this temperature in shorter time. This mechanism appears to be consistent with experimental results; the precipitation of Ti-rich plates occurs at temperatures in the range from  $\sim 315^\circ\text{C}$  to above  $600^\circ\text{C}$  in neutron irradiation studies [6-10,18] and at temperatures usually  $>600^\circ\text{C}$  in unirradiated thermal aging studies [4,5,12,14]. The lower temperature limit and minimum time at temperature for precipitation of the Ti-rich plates have not been established in unirradiated annealing studies.

## REFERENCES

1. A.L. Qualls and T. Muroga, J. Nuclear Materials, **258-263**, (1998), p. 407.
2. S.J. Zinkle, "Summary of the U.S. Specimen Matrix for the HFIR 13J Varying Temperature Irradiation Capsule," Fusion Materials Semiannual Progress Report, DOE/ER-0313/23, December 1997, p. 352.
3. A.L. Qualls, "Summary of the Operation of the Varying Temperature Experiment," Fusion Materials Semiannual Progress Report, DOE/ER-0313/28, June 2000, p. 266.
4. B.A. Pint, P.M. Rice, L.D. Chitwood, J.H. DeVan, and J.R. DiStefano, "Microstructural Characterization of External and Internal Oxide Products on V-4Cr-4Ti," Fusion Materials Semiannual Progress Report, DOE/ER-0313/24, June 1998, p. 77.
5. M.L. Grossbeck, J.F. King, D.J. Alexander, P.M. Rice, and G.M. Goodwin, J. Nuclear Materials, **258-263**, (1998), p. 1369.
6. P.M. Rice and S.J. Zinkle, J. Nuclear Materials, **258-263**, (1998), p. 1414.
7. D.S. Gelles and H.M. Chung, "Microstructural Examination of Irradiated Vanadium Alloys," Fusion Materials Semiannual Progress Report, DOE/ER-0313/21, December 1996, p. 79.
8. H.M. Chung, J.Gazda, and D.L. Smith, "Irradiation-Induced Precipitation and Mechanical Properties of Vanadium Alloys at  $<430^\circ\text{C}$ ," Fusion Materials Semiannual Progress Report, DOE/ER-0313/24, June 1998, p. 49.
9. S. Ohnuki, D.S. Gelles, B.A. Loomis, F.A. Garner, and H. Takahashi, J. Nuclear Materials, **179-181**, (1991), p. 775.
10. M. Satou, K. Abe, H. Kyano, and H. Takahashi, J. Nuclear Materials, **191-194**, (1992), p. 956.

11. D.S. Gelles, P.M. Rice, S.J. Zinkle, and H.M Chung, *J. Nuclear Materials*, **258-263**, (1998), p. 1380.
12. J. Bentley and B. Pint, "Analytical Electron Microscopy of V-4%Ti-4%Cr Alloys, to be published in the proceedings of the Microscopy Society of America, (2001).
13. J.W. Edington, in "Practical Electron Microscopy in Materials Science," N.V. Philips' Gloeilampenfabrieken, Eindhoven, 1975.
14. K.H. Kramer, *J. Less-Common Metals*, **21**, (1970), p. 365
15. D.T. Hoelzer, "Structural Analysis of Ti-oxycarbonitrides in V-Cr-Ti Base Alloys," Fusion Materials Semiannual Progress Report, DOE/ER-0313/25, December 1998, p. 59.
16. D.T. Hoelzer, Unpublished results, (2000).
17. R.E. Gold, D.L. Harrod, R.L. Ammon, R.W. Buckman, Jr., and R.C. Svedberg, in Technical Assessment of Vanadium-Base Alloys for Fusion Reactor Applications, Final Report prepared by Westinghouse Electric Corp. under Contract EG-77-C-02-4540 for the Department of Energy, Office of Fusion Energy, (1978).
18. R. Carlander, S.D. Harkness, and A.T. Santhanam, "Effects of Radiation on Substructure and Swelling Behavior of Vanadium Alloys," ASTM STP 529, 1973, p. 399.